ACS Chemical Neuroscience

Research Article

pubs.acs.org/chemneuro

Pharmacological Characterization of the Newly Synthesized 5-Amino-*N*-butyl-2-(4-ethoxyphenoxy)-benzamide Hydrochloride (BED) as a Potent NCX3 Inhibitor That Worsens Anoxic Injury in Cortical Neurons, Organotypic Hippocampal Cultures, and Ischemic Brain

Agnese Secondo,[†,∥] Giuseppe Pignataro,[†,∥] Paolo Ambrosino,[†] Anna Pannaccione,[†] Pasquale Molinaro,[†] Francesca Boscia,[†] Maria Cantile,[†] Ornella Cuomo,[†] Alba Esposito,[†] Maria Josè Sisalli,[†] Antonella Scorziello,[†] Natascia Guida,[‡] Serenella Anzilotti,[‡] Ferdinando Fiorino,[§] Beatrice Severino,[§] Vincenzo Santagada,[§] Giuseppe Caliendo,[§] Gianfranco Di Renzo,[†] and Lucio Annunziato*[,†,‡]

[†]Department of Neuroscience, Reproductive and Odontostomatological Sciences, School of Medicine, "Federico II" University of Naples, Via Pansini 5, 80131 Naples, Italy

[‡]IRCCS SDN, Naples, Italy, [§]Department of Pharmacy, "Federico II" University of Naples, Via D. Montesano 49, 80131 Naples, Italy

ABSTRACT: The Na^+/Ca^{2+} exchanger (NCX), a 10-transmembrane domain protein mainly involved in the regulation of intracellular Ca^{2+} homeostasis, plays a crucial role in cerebral ischemia. In the present paper, we characterized the effect of the newly synthesized compound 5-amino-*N*-butyl-2-(4-ethoxyphenoxy)-benzamide hydrochloride (BED) on the activity of the three NCX isoforms and on the evolution of cerebral ischemia. BED inhibited NCX isoform 3 (NCX3) activity (IC_{50} = 1.9 nM) recorded with the help of single-cell microflorimetry, $^{45}Ca^{2+}$ radiotracer fluxes, and patch-clamp in whole-cell configuration. Furthermore, this drug displayed negligible effect on NCX2, the other isoform expressed within the CNS, and it failed to modulate the ubiquitously expressed NCX1 isoform. Concerning the molecular site of action, the use of chimera strategy and deletion mutagenesis showed that α1 and α2 repeats of NCX3 represented relevant molecular determinants for BED inhibitory action, whereas the intracellular regulatory f-loop was not involved. At 10 nM, BED worsened the damage induced by oxygen/glucose deprivation (OGD) followed by reoxygenation in cortical neurons through a dysregulation of $[Ca^{2+}]_i$. Furthermore, at the same concentration, BED significantly enhanced cell death in CA3 subregion of hippocampal organotypic slices exposed to OGD and aggravated infarct injury after transient middle cerebral artery occlusion in mice. These results showed that the newly synthesized 5-amino-*N*-butyl-2-(4-ethoxyphenoxy)-benzamide hydrochloride is one of the most potent inhibitor of NCX3 so far identified, representing an useful tool to dissect the role played by NCX3 in the control of Ca^{2+} homeostasis under physiological and pathological conditions.

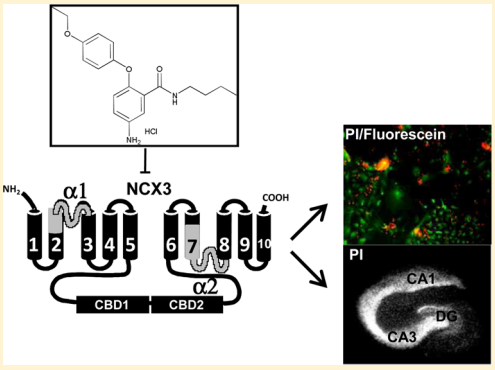

KEYWORDS: *Sodium calcium exchanger, NCX isoforms, NCX3 inhibitor, cerebral ischemia, OGD*

A great deal of interest has been devoted to the discovery of clinically effective drugs against cerebral ischemia, and of pharmacological tools able to identify potential drugable targets in this relevant and frequently observed neurological disease. Interestingly, the modulation of the Na^+/Ca^{2+} exchanger (NCX)[1,2] seems to modify the course of the disease. In fact, either the specific knock-down or gene ablation of ncx leads to a worsening of brain damage and neurological deficits induced in mice and rats by experimentally induced focal ischemia.[3,4] NCX is a 10-transmembrane domain protein[5] that couples the efflux of Ca^{2+} to the influx of Na^+ into the cell or viceversa by operating in a bidirectional way. NCX family belongs to a Cation/Calcium Exchanger Superfamily that includes four other families. Three different genes coding for the three different NCX1,[6] NCX2,[7] and NCX3[8] proteins have been identified in mammals. All these three isoforms share the same topology with the amino terminus located in the extracellular space, and the carboxyl terminus located in the intracellular space. The 10-transmembrane segments can be divided into an N-terminal hydrophobic domain and into a C-terminal hydrophobic domain, each composed of 5 TMSs. Each group of 5 TMSs is separated from the other through a large hydrophilic intracellular loop of 550 amino acids, named f loop[9] that is not implicated in Na^+ and Ca^{2+} translocation, but is responsible for the regulation of NCX activity. Interestingly,

Received: January 30, 2015
Revised: April 14, 2015
Published: May 5, 2015

DOI: 10.1021/acschemneuro.5b00043
ACS Chem. Neurosci. 2015, 6, 1361−1370

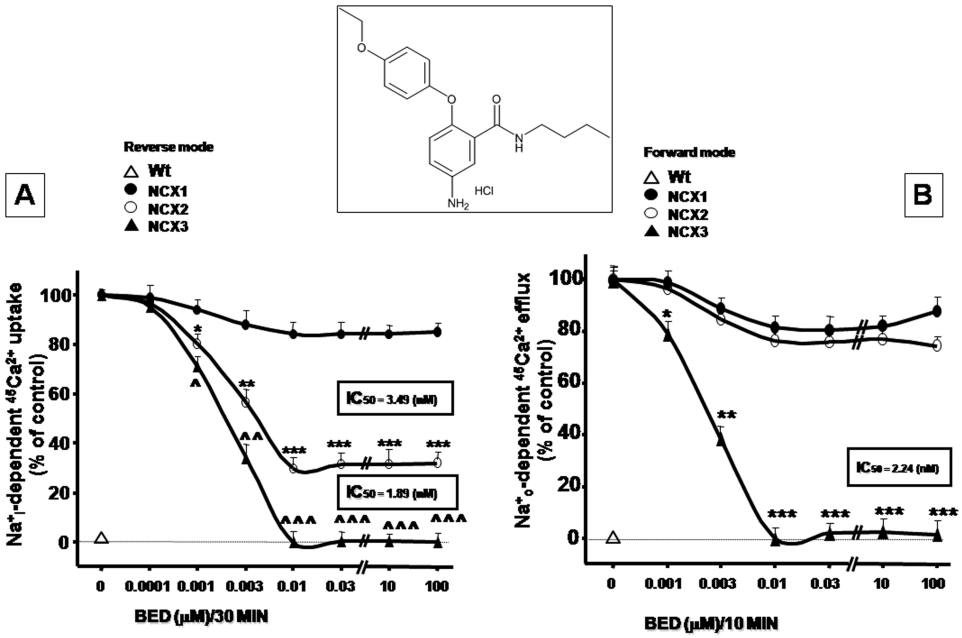

Figure 1. Dose–response curves of the effects of BED on NCX working in the reverse and forward mode of operation in BHK cells expressing distinctly the three NCX isoforms. Top: Chemical structure of BED. (A) BED was applied for 30 min on BHK cells stably transfected with NCX1, NCX2, or NCX3, and then Na^+-dependent $^{45}Ca^{2+}$ uptake was evaluated. Data obtained in BHK cells stably transfected with NCX1, NCX2, or NCX3 are presented as percentage of the control values obtained in the absence of the drug (control). Data of Na^+-dependent $^{45}Ca^{2+}$ uptake in BHK-Wt was also reported. Values represent means ± SEM (n = 4 experimental sessions). *p < 0.05 versus its respective control; **,***p < 0.05 versus previous concentrations; ^p < 0.05 versus its respective control; ^^,^^^p < 0.05 versus previous concentrations and the same concentration on NCX2. (B) BED was applied for 10 min on BHK cells stably transfected with NCX1, NCX2, or NCX3, and then Na^+-dependent $^{45}Ca^{2+}$ efflux was evaluated. Data obtained in BHK cells stably transfected with NCX1, NCX2, or NCX3 are presented as percentage of the control values obtained in the absence of the drug (control). Data of Na^+-dependent $^{45}Ca^{2+}$ efflux in BHK-Wt was also reported. Values represent means ± SEM (n = 4 experimental sessions). *p < 0.05 versus its control and the same concentration on NCX1 and NCX2. **, ***p < 0.05 versus previous concentrations.

this function is elicited by several cytoplasmic messengers and transductional mechanisms, such as Ca^{2+} and Na^+ ions, nitric oxide (NO),[10] phosphatydilinositol 4,5-bisphosphate (PIP2), protein kinase C (PKC), protein kinase A (PKA), phosphoarginine (PA), and adenosine trisphosphate (ATP).[2] After the discovery of NCX activity in 1969, studies have reported that some compounds can interfere with this antiporter.[11,12] In the last 35 years, in fact, several inorganic and organic compounds have been reported to activate or block the NCX activity. However, the selectivity of this action has often been questioned.[2] Since then, in an attempt to evaluate NCX activity, amiloride has been used as a probe to block NCX function.[12] However, two major drawbacks have limited its use. First, millimolar concentrations are required for its NCX inhibitory activity; second, it lacks specificity, since it can also inhibit both the epithelial Na^+ channel at micromolar concentrations and the Na^+/H^+ exchanger in the millimolar range. Later on, in order to overcome the lack of selectivity and to increase the potency of this drug, additional compounds belonging to ethoxyanilines, quinazolinone, thiazolidine, phenoxypyridine, ylacetamide, benzofuran, and imidazoline derivatives were produced by conventional chemical synthesis. However, these newly synthesized compounds although provided with a higher potency did not display the expected selectivity on the mode of operation of the antiporter and on the different isoforms and splicing variants. In the present paper we characterize the molecular mechanism of the new compound 5-amino-*N*-butyl-2-(4-ethoxyphenoxy)-benzamide hydrochloride (BED), whose synthesis has been conducted with an approach already published.[13] In particular, we examined the effect of this compound on the activity of NCX isoforms and on the evolution of cerebral ischemia experimentally modeled in vitro and in vivo, a complex pathological process which requires a tight control of Ca^{2+} and Na^+ homeostasis through NCX.

RESULTS

Effect of BED on NCX1, NCX2, and NCX3 Activity Evaluated as Na^+-Dependent $[Ca^{2+}]_i$ Increase, Na_0^+-Dependent $^{45}Ca^{2+}$ Efflux, Na_i^+-Dependent $^{45}Ca^{2+}$ Uptake and by Patch-Clamp Technique in Stably Transfected BHK-NCX1, BHK-NCX2, and BHK-NCX3 Cells. In order to evaluate the effect on each isoform of the exchanger of BED, whose structure has been reported at the top of Figure 1, NCX activity was assessed as Na_i^+-dependent $^{45}Ca^{2+}$ uptake and Na_0^+-dependent $^{45}Ca^{2+}$ efflux in stably transfected BHK-NCX1, BHK-NCX2 and BHK-NCX3 cells in the presence of different concentrations of the biphenyl ether derivative and in BHK Wild type (BHK-Wt) (Figure 1). As a matter of course, Na^+-free solution failed to produce Na_i^+-dependent $^{45}Ca^{2+}$ uptake in BHK-Wt cells (Figure 1A). However, in stably transfected BHK-NCX1, BHK-NCX2, and BHK-NCX3 cells, the effect of BED was evaluated on the maximum rate of NCX activation (100%) elicited by Na^+-free. BED was able to reduce the reverse mode of operation of NCX2 and NCX3, but not of NCX1, in a dose-dependent manner with the following IC_{50}: 3.49 nM for NCX2 and 1.89 nM for NCX3 (Figure 1A). The ability of BED to reduce $^{45}Ca^{2+}$ efflux was also studied by using

DOI: 10.1021/acschemneuro.5b00043
ACS Chem. Neurosci. 2015, 6, 1361−1370

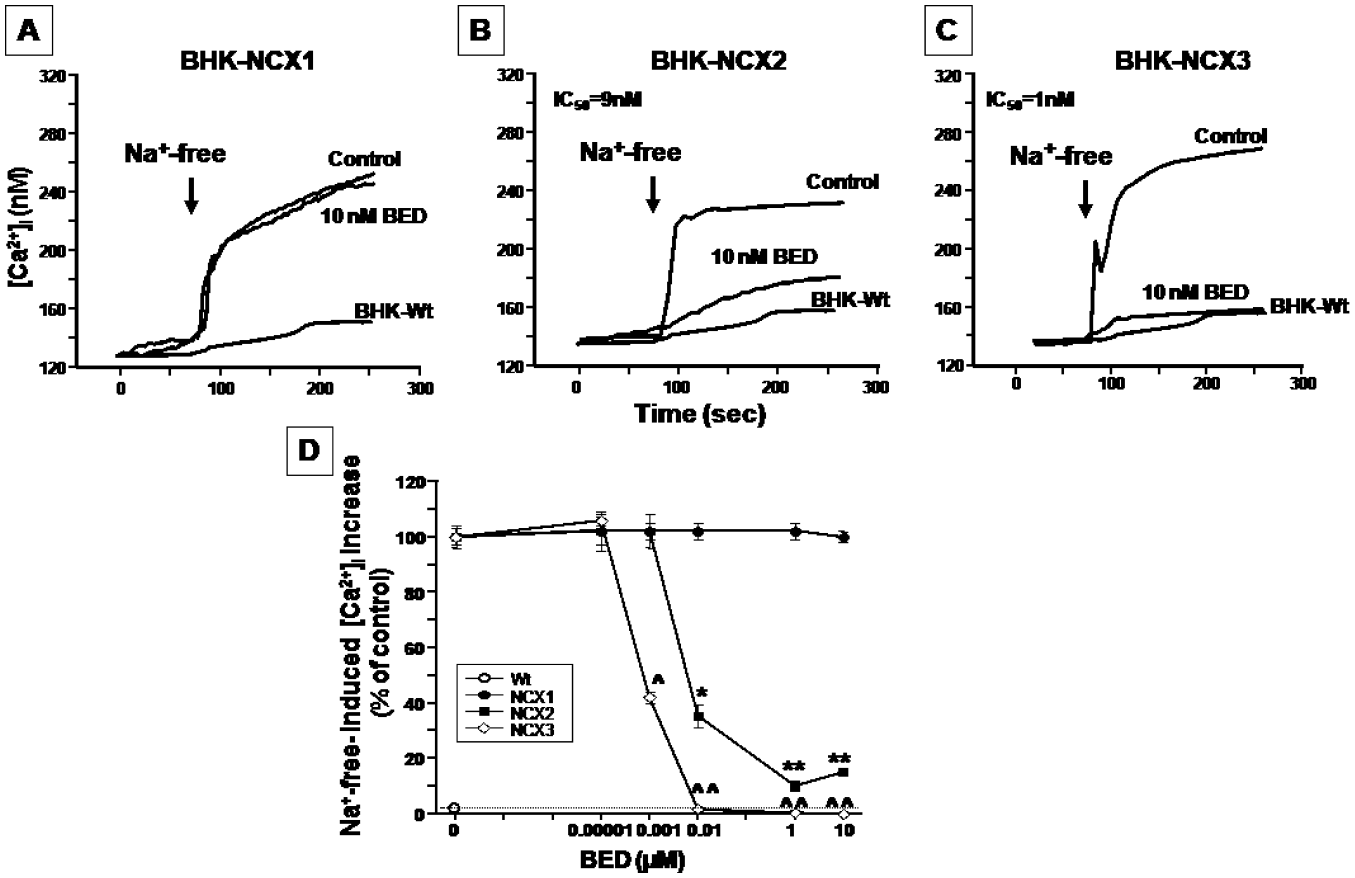

Figure 2. Effect of BED on Na^+-free-induced $[Ca^{2+}]_i$ increase in BHK-Wt, BHK-NCX1, BHK-NCX2, and BHK-NCX3 cells. Top: Typical superimposed traces representing the effect of Na^+-free on $[Ca^{2+}]_i$ in BHK-Wt and in the absence or presence of the drug in (A) BHK-NCX1, (B) BHK-NCX2, and (C) BHK-NCX3 cells. Bottom: (D) Dose−response curve of the effect of BED on Na^+-free- induced NCX activity. BED, at the indicated concentrations, was added 10 min before Na^+-free application. Values represent means ± SEM of three different experiments. The percentage of $[Ca^{2+}]_i$ increase after Na^+-free perfusion was calculated as Δ% of plateau/basal value. For each of the three experiments, 10−20 individual cells were monitored. *$p < 0.05$ versus its control group; **$p < 0.05$ versus its previous concentrations and control; ^$p < 0.05$ versus its control group; ^^$p < 0.05$ versus its previous concentrations, control, and the same concentration on NCX2.

Ca^{2+}-free-Na^+ containing solution plus 2 mM EGTA, as reported in Methods. Cells were exposed to the above-mentioned solution for 10 s, a time in which no efflux was detected in BHK Wild type cells (Figure 1B). Interestingly, only the forward mode of NCX3 was reduced by the drug in a dose-dependent manner with an IC_{50} of 2.24 nM (Figure 1B). Furthermore, NCXs activity was also studied by Fura-2AM video-imaging on single-cell as Na^+ gradient-dependent $[Ca^{2+}]_i$ increase elicited by a single pulse of Na^+-deficient $NMDG^+$ medium (Na^+-free). To dissect $[Ca^{2+}]_i$ increase due to NCX component from the other contributors, cells were treated with thapsigargin, a specific and irreversible inhibitor of the sarco(endo)plasmic reticulum ATPase SERCA. Before perfusion, cells were exposed for 10 min to thapsigargin (1 μM) in order to deplete the endoplasmic reticulum (ER) and to prevent Ca^{2+} refilling into ER upon Na^+-free administration. With this protocol, thapsigargin did not interfere with Na^+-free-induced NCX activation (data not shown). In BHK-NCX3 and BHK-NCX2 cells, Na^+-free perfusion caused a rapid rise in $[Ca^{2+}]_i$ through the reverse mode of operation that was reduced by BED in dose dependent way (0.00001−10 μM) with the IC_{50}'s of 1 nM for NCX3 and 9 nM for NCX2, respectively (Figure 2). As a matter of course, Na^+-free solution failed to elicit $[Ca^{2+}]_i$ rise in wild-type BHK cells (BHK-Wt) (Figure 2), which lacked all three NCX isoforms.[14] Furthermore, the effect of BED on NCX1, NCX2, and NCX3 activity was more directly assessed by the patch-clamp technique in whole cell configuration in stably transfected BHK cells. The whole-cell current was measured at +60 and −120 mV using the ramp-clamp protocol (see Methods). To isolate NCX currents (I_{NCX}), cells were recorded for 5 min with the well-known NCX inhibitor $NiCl_2$ (5 mM). The Ni^{2+}-sensitive component, representing the isolated I_{NCX}, was obtained as previously reported.[15] No current corresponding to I_{NCX} was recorded in BHK-Wt cells (Figure 3). The incubation with BED strongly inhibited both the outward (reverse mode) and inward (forward mode) direction of I_{NCX3} in dose-dependent way with the following IC_{50}: 0.62 nM for NCX3 reverse mode and 1.01 nM for NCX3 forward mode. However, only the reverse mode of operation of NCX2 was affected by the drug with an IC_{50} of 1.08 nM (Figure 3). The IC_{50} of BED on NCX3 reverse and forward modes of operation were compared with those of 3-amino-6-chloro-5-[(4-chloro-benzyl)amino]-*N*-[[(2,4-dimethylbenzyl)amino]iminomethyl]-pyrazinecarboxamide (CB-DMB) (Table 1). BED, in the same experimental conditions, showed a higher potency than CB-DMB in inhibiting NCX3 activity (Table 1). Furthermore, BED inhibited also TTX-sensitive Na^+ currents recorded in GH3 cells with an IC_{50} of 8.1 μM while CB-DMB inhibited TTX-sensitive Na^+ currents with an IC_{50} of 1.6 μM.[15]

DOI: 10.1021/acschemneuro.5b00043
ACS Chem. Neurosci. 2015, 6, 1361−1370

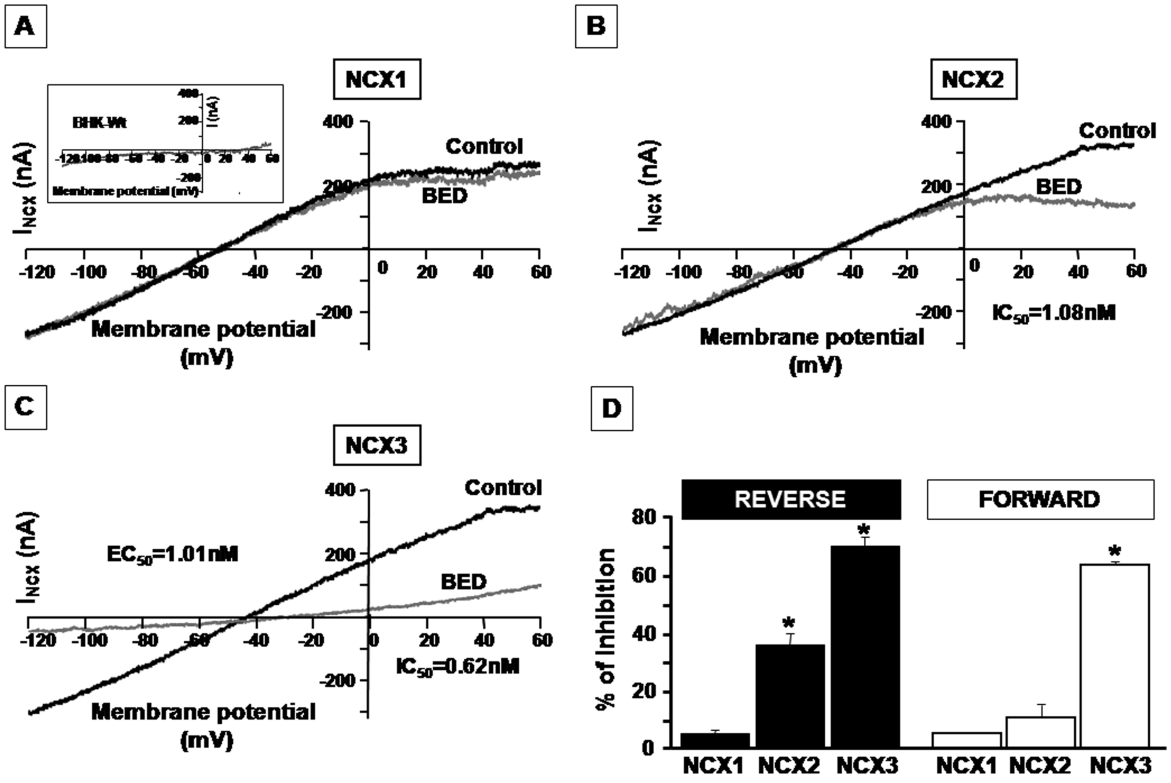

Figure 3. Effect of BED on I_{NCX} recorded in the reverse mode of operation in BHK-Wt and BHK cells stably transfected with NCX1, NCX2, or NCX3. I_{NCX} was recorded from BHK-Wt, BHK-NCX1, BHK-NCX2, and BHK-NCX3 cells by the patch-clamp technique in whole-cell configuration. Currents were recorded as reported in Methods. I_{NCX} superimposed traces recorded from (A) BHK-NCX1, (B) BHK-NCX2, and (C) BHK-NCX3 cells under control conditions (black trace) and after 10 min preincubation with the drug (gray trace, 10 nM). (D) quantification of I_{NCX} in the presence of BED reported as percent of current inhibition. For each experiment, 4−10 individual cells were monitored. *$p < 0.05$ versus each respective control.

Table 1. Effect of BED on NCX Reverse and Forward Mode of Operation, Comparison with the Previously Characterized NCX Inhibitor CB-DMB

	BED (IC_{50}, nM)		CB-DMB (IC_{50}, nM)[15]	
	reverse	forward	reverse	forward
Fura-2AM	1		177	
$^{45}Ca^{2+}$	1.89	2,24	420	600
patch-clamp	0.62	1,01	230	260

Effect of BED in NCX1, NCX2, and NCX3 Mutants Lacking "f-loop" or NCX1/NCX3 Chimeras Assessed by Na^+-Dependent $[Ca^{2+}]_i$ Increase and Na_i^+-Dependent $^{45}Ca^{2+}$ Uptake in Stably Transfected BHK Cells. To investigate the molecular determinants of BED on the molecular structure of NCX3 isoform, the intracellular f-loop, a region mainly involved in the regulation of NCX function, was deleted in NCX3 cDNA (NCX3Δf) (Figure 4A). Interestingly, Fura 2-AM single-cell video-imaging experiments revealed that the elimination of the f-loop did not produce any change in the action profile exerted by the biphenyl ether derivative on NCX3 activity (Figure 4B). In fact, Na^+-free perfusion caused a rapid rise in $[Ca^{2+}]_i$ that was reduced in the presence of BED by the same extent in both NCX3Δf and in NCX3 wild type (Figure 4). These data suggested the existence of an inhibitory site located outside the intracellular f-loop of NCX3 structure. To establish the site responsible for BED-mediated down-regulation of NCX3 activity, we generated four chimeras between NCX3 and NCX1 taking advantage on their different sensitivity to BED. Particularly, the effect of BED was studied in N3-227/469 and N3-707/776 chimeras obtained by substituting the BED-insensitive NCX1 regions 227/469 and 707/776 with the homologous segments in NCX3 structure. Fura-2 microfluorimetry showed that the activity in the reverse mode of these two chimeras was inhibited by BED (10 nM) in the same extent as NCX3 Wt (Figure 4C,D). In fact, Na^+-free perfusion caused a rapid rise in $[Ca^{2+}]_i$ that was reduced in the presence of BED (10 nM) in both in N3-227/469 and N3-707/776 chimeras as well as in NCX3 wild type (Figure 4G). Finally, we substituted the NCX3 region corresponding to the α1 repeat with the homologous 143−167 segment of NCX1, thus producing the chimera named N3-143/167 (Figure 4E). Furthermore, a chimera between NCX3 and NCX1, named N3-777/818, was produced by introducing in the NCX3 region, corresponding to the α_2 repeat, the homologous NCX1 sequence 777/818 (Figure 4F). Fura-2 microfluorimetry showed that the activity of these two chimeras was not affected by BED (10 nM) (Figure 4G). In fact, Na^+-free perfusion caused a rapid rise in $[Ca^{2+}]_i$ that remained unchanged in the presence of BED (10 nM) in both N3-143/167 and N3-777/818 chimeras (Figure 4E−G). The effect of BED on NCX activity was also determined in the previous described mutant and chimeras by means of Na^+-dependent $^{45}Ca^{2+}$ uptake in the presence of 10 nM of the biphenyl ether derivative (Figure 4H). BED was able to significantly inhibit Na^+-dependent $^{45}Ca^{2+}$ uptake in NCX3Δf and in N3-227/469 and N3-707/776 chimeras as well as in NCX3 Wt, while it failed to change Na^+-dependent $^{45}Ca^{2+}$ uptake in N3-143/167 and N3-777/818

DOI: 10.1021/acschemneuro.5b00043
ACS Chem. Neurosci. 2015, 6, 1361−1370

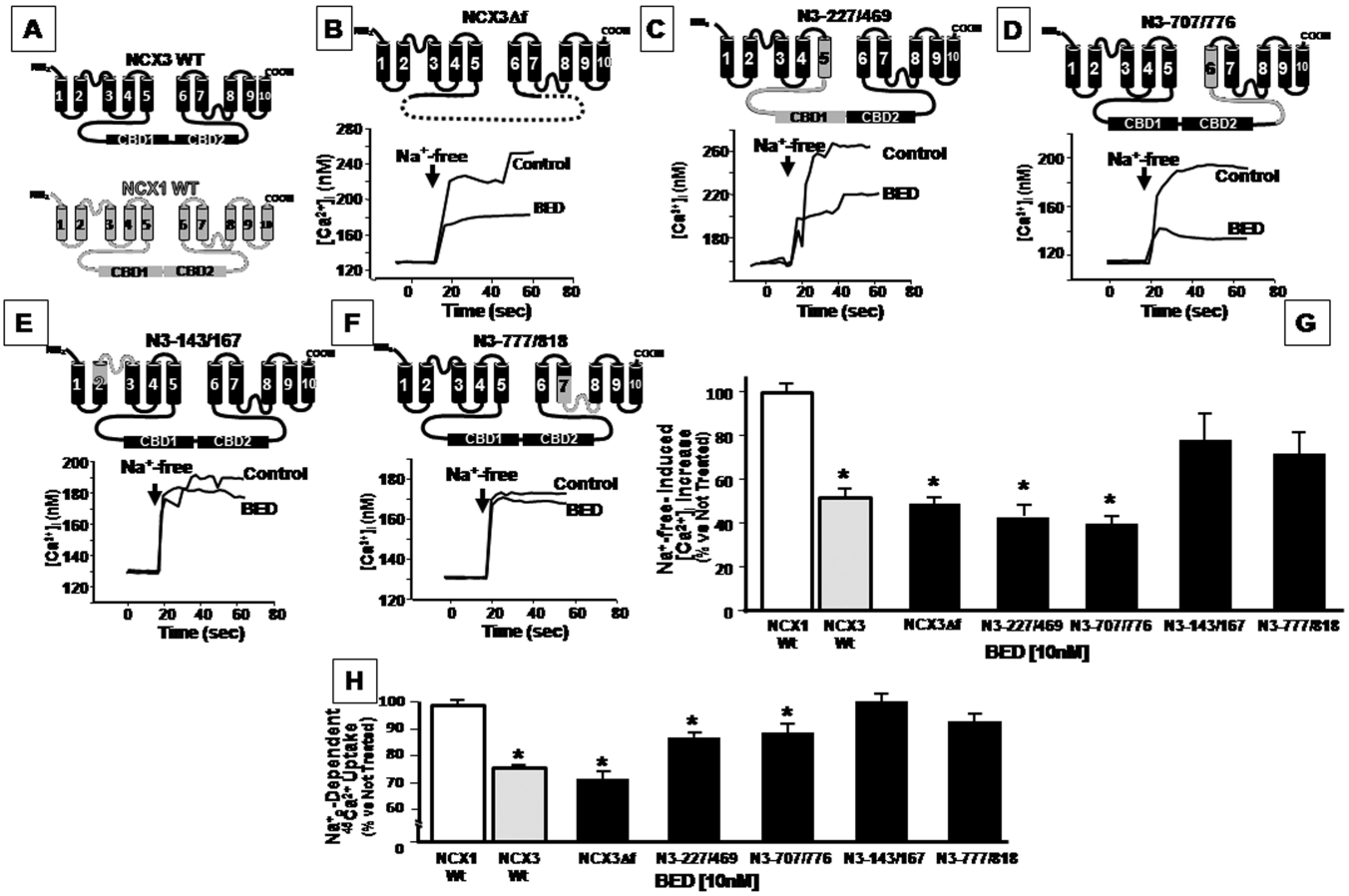

Figure 4. Effect of BED on NCX3/NCX1 chimera and NCX3Δ*f*mutant. (B−F) typical superimposed traces representing the effect of Na^+-free alone and Na^+-free + BED (10 nM) on $[Ca^{2+}]_i$ in N3-227/469, N3-707/776, N3143/167, and N3-777/818 chimeras and in NCX3Δf mutant, whose structure derives from NCX1 and NCX3 (A). (G) Quantification of the effect of the drug (10 nM) on $[Ca^{2+}]_i$ increase induced by Na^+-Free in BHK-NCX3 and BHK-NCX1 wild type (Wt) cells, in the above-mentioned mutants. Each bar represents the mean (±SEM) of the values obtained in three independent experimental sessions. For each experiment, 40−65 individual cells were monitored. *$p < 0.05$ versus its respective control. (H) Quantification of the effect of the drug (10 nM) on Na^+-dependent $^{45}Ca^{2+}$ uptake in the same experimental conditions depicted in (A). Each bar represents the mean (±SEM) of the values obtained in four independent experimental sessions. *$p < 0.05$ versus its control.

chimeras (Figure 4H). This suggested that both the α_1 and α_2 regions of NCX3 were involved in the inhibitory efficacy of the biphenyl ether derivative.

Effect of BED on Neuronal Survival in Organotypic Hippocampal Cultures Exposed to Oxygen/Glucose Deprivation (OGD). The exposure of hippocampal organotypic slices to OGD in the presence of 0.01 μM BED significantly enhanced cell death in CA3 subregion compared to OGD itself, as demonstrated by the increase in PI uptake (Figure 5A−D). However, no significant effect of BED exposure was observed in CA1 and DG hippocampal subregions exposed to OGD (Figure 5B,C). The more severe cell death observed in CA3 subregion as compared to CA1 and DG upon BED exposure might be due to the blockade of NCX3 in that regions where this exchanger isoform is greater expressed.[3,16] The presence of higher BED concentration (10 μM) in the incubation media per se did not affect neuronal viability in this preparation (Figure 5B−D).

Effect of BED on $[Ca^{2+}]_i$ and Cell Survival of Cortical Neurons Exposed to OGD Plus Reoxygenation and on Infarct Volume in Mice Subjected to tMCAo. Primary cortical neurons treated with 10 nM BED and exposed to 2 h OGD followed by 24 h reoxygenation displayed a significant increase in $[Ca^{2+}]_i$ as compared to OGD followed by reoxygenation alone (Figure 6A) and vehicle treated group. Furthermore, the addition of 10 nM BED enhanced cell death induced by 2 h OGD followed by 24 h reoxygenation (Figure 6B). On the other hand time-course experiments, evaluating basal toxicity of BED on BHK-NCX3 cells, showed that this drug did not induce any toxicity even at 100 μM (data not shown). Moreover, BED icv administered (1 μL) at a concentration of 500 nM dramatically increased the extent of the ischemic lesion in C57/BL6 male mice subjected to 60 min of MCAO followed by 24 h of reperfusion as compared to vehicle administered mice (percent of ischemic damage was 21.0 ± 0.8 in the vehicle treated group and 39.1 ± 1.6 in the BED treated group, respectively) (Figure 6C). Particularly, the enlargement of the ischemic core in these mice was particularly evident in the more peripheral temporoparietal cortex (9.36 ± 0.9 vs 28.36 ± 1.6) (Figure 6C).

■ DISCUSSION

In the present study, we report the characterization of the newly synthesized compound 5-amino-*N*-butyl-2-(4-ethoxyphenoxy)-benzamide hydrochloride, named BED, as a new selective NCX3 inhibitor. Furthermore, the effect of BED on the neuronal damage induced by in vitro and in vivo cerebral ischemia was also examined. As concerns the chemical structure

DOI: 10.1021/acschemneuro.5b00043
ACS Chem. Neurosci. 2015, 6, 1361−1370

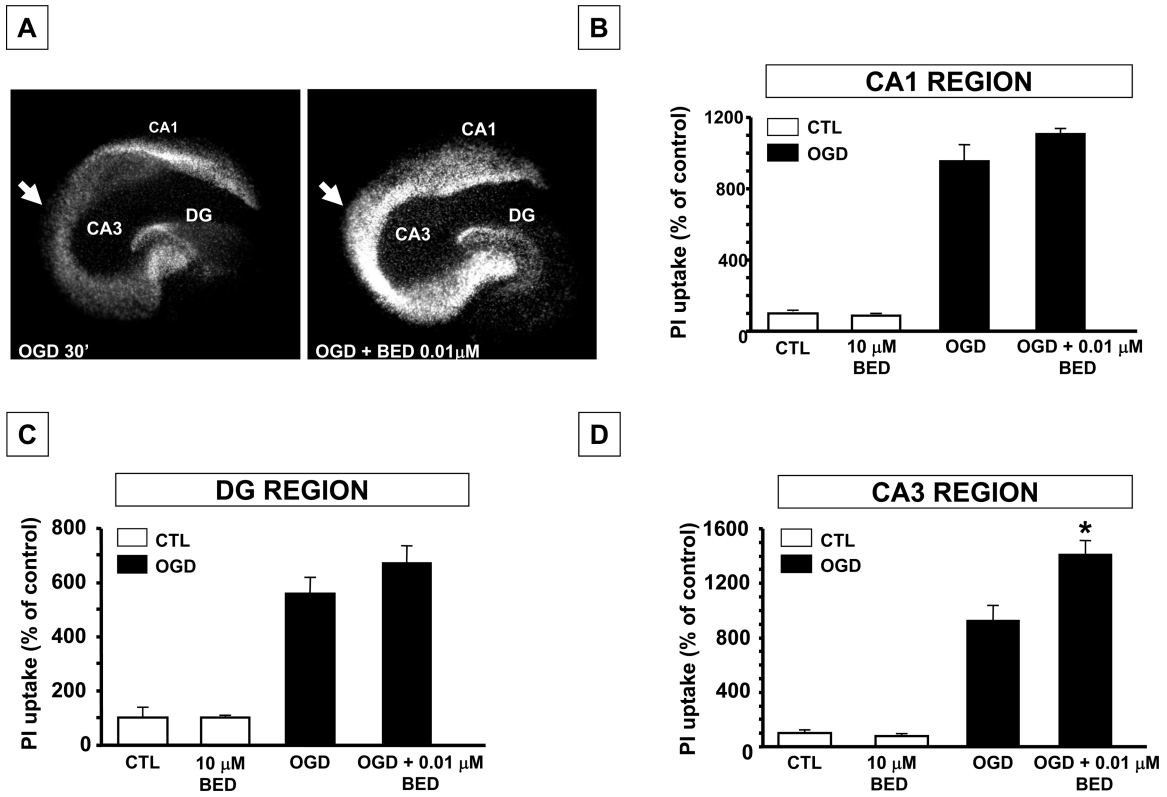

Figure 5. Effect of BED on cell death in CA1, CA3, and DG subregions of organotypic hippocampal cultures exposed to hypoxic conditions. (A) PI fluorescence staining pattern observed in a representative organotypic hippocampal cultures (OHSCs) exposed to 25 min of OGD followed by 24 h of reoxygenation. (B−D) quantification of the cell damage in selected hippocampal subregions, CA1, DG, and CA3 evaluated by densitometric analysis of PI fluorescence. PI fluorescence intensity recorded in each hippocampal subfield was normalized to that recorded in the respective subregion of untreated OHSCs. All the values of the experimental groups were expressed as percentage of PI fluorescence. Each data point is the mean ± SEM of the data obtained from 20−24 OHSCs in three separate experiments. Scale bar in (A): 400 μm. *$p < 0.05$ versus all the other groups.

of the newly synthesized compound, BED was drawn taking into consideration the chemical structure of a well-known NCX inhibitor, SEA0400.[17] In particular, compared with the SEA0400 structure, the biphenyl ether moiety was maintained unaltered. In addition, two new groups, an amino group and an amide group, were inserted on one of the two benzene rings. These chemical modifications have produced dramatic changes in the biological activity of this compound, determining a high NCX3 isoform selectivity and potency never found in any other NCX inhibitor so far described. In fact, the potency of BED (i.e., IC_{50} = 1 nM) is significantly higher than that of the amiloride derivative 3-amino-6-chloro-5-[(4-chloro-benzyl)-amino]-*N*-[[(2,4-dimethylbenzyl)amino]iminomethyl]-pyrazinecarboxamide (CB-DMB)[15] used as reference drug in the present study and of the new isothyourea derivative YM-244769 which is the most potent available NCX3 inhibitor working in the nanomolar range.[18] However, YM-244769 inhibits NCX3 only in the reverse mode of operation, whereas BED inhibits NCX3 when it acts bidirectionally. Interestingly, the substitution on the amino group with an acetamide group abolishes the effect on NCX (data not shown), thus showing that the amino group plays an important role in the inhibitory effect exerted by the newly synthesized drug. The use of deletion mutagenesis showed that the intracellular f-loop of NCX3, which is involved in the activity regulation of the antiporter,[2,19] is not involved in BED inhibitory action. In contrast, the use of NCX1/NCX3 chimeras revealed that both the α_1 and α_2 repeats were mainly involved in BED inhibitory action. Interestingly, these regions represent common molecular determinants required for nitric oxide to downregulate NCX3 activity,[9] for neurounina-1 to increase[20] NCX1, and for KB-R7943, SEA0400, and SN-6 to block[21] NCX1. Accordingly, the substitution of these BED-sensitive regions of NCX3 with the corresponding BED-insensitive regions of NCX1 prevented the inhibitory effect exerted by the drug on NCX3. This suggests that the molecular determinant of NCX3 was found outside the f-loop, at the level of both the α_1 and α_2 repeats. As concerns the selectivity of BED against other channels, our results showed that this drug inhibited TTX-sensitive Na^+ currents with an IC_{50} of 8.1 μM that was significantly larger than that recorded for NCX3 blockade. However, the inhibition of voltage-gated Na^+ channels should prevent instead of worsen hypoxia-induced neuronal injury, thus suggesting that the detrimental effects of the drug on neuronal viability may be ascribe to the most prominent blockade of NCX3 activity. In this respect, we have previously demonstrated that either the specific knock-down or gene ablation of ncx3 leads to a worsening of brain damage and neurological deficits induced in mice and rats by experimentally induced focal ischemia.[3,4] The present results obtained with BED on ischemic brain volumes was in line with the above-mentioned results and with those obtained in primary neurons derived from $ncx3^{-/-}$ mice subjected to OGD.[4] In the present study, the administration of the drug during the OGD phase rendered cortical neurons more vulnerable to the reoxygenation phase as occurs for $ncx3^{-/-}$ cortical neurons compared with $ncx3^{+/+}$ neurons when

DOI: 10.1021/acschemneuro.5b00043
ACS Chem. Neurosci. 2015, 6, 1361−1370

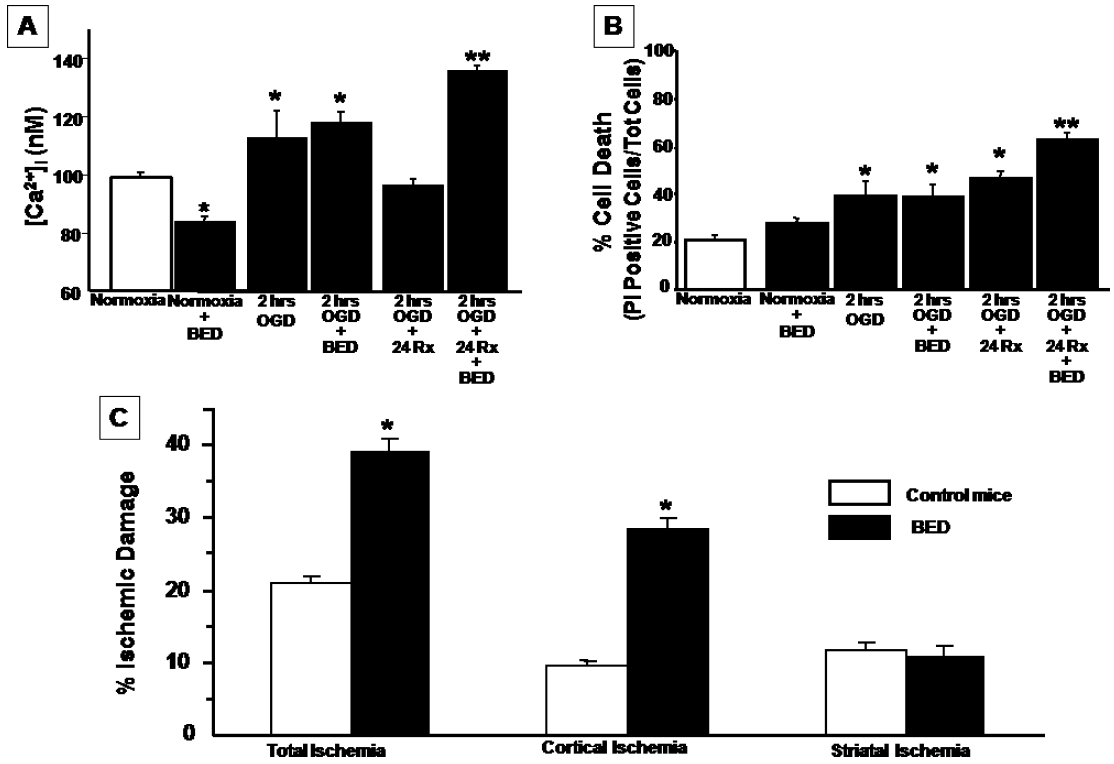

Figure 6. Effect of BED on $[Ca^{2+}]_i$ and cell survival of primary cortical neurons exposed to oxygen and glucose deprivation (OGD) plus reoxygenation and evaluation of infarct volume induced by tMCAo in C57/BL6 male treated with BED. (A) $[Ca^{2+}]_i$ in cortical neurons (7−10 DIV (days in vitro)) under normoxic conditions, pretreated with 10 nM BED and then exposed to 24 h normoxia, exposed to 2 h OGD followed by 24 h reoxygenation, or pretreated with 10 nM BED and then exposed to 2 h OGD followed by 24 h reoxygenation. Values represent means ± SEM of three different experiments. For each of the experiments, 11−25 individual cells were monitored. *$p < 0.05$ versus control group; **$p < 0.05$ versus all. (B) Cell death quantification was performed by PI and fluorescein dyes in 7−10 DIV cortical neurons exposed to 24 h normoxia, pretreated with 10 nM BED and then exposed to 24 h normoxia, exposed to 2 h OGD followed by 24 h reoxygenation, or pretreated with 10 nM BED and then exposed to 2 h OGD followed by 24 h reoxygenation. At the end of the experiments, cells were stained with PI and fluorescein and images were acquired as reported in Methods. Each bar represents the mean ± SEM of three different experimental values studied in three independent experimental sessions. The data are reported as percent of cell death occurring in each group as compared with their respective normoxic cells. *$p <$ 0.05 versus normoxia and normoxia+BED; **$p < 0.05$ versus all. (C) Effect of the drug on infarct volume evaluated by 2,3,5-triphenyl tetrazolium chloride (TTC) staining in C57/BL6 male mice subjected to tMCAo. Each column represents the mean ± SEM of the percent of the infarct volume compared to the ipsilateral hemisphere ($n = 9$ animals for each group). Ischemic mice were euthanized 24 h after tMCAo. *$p < 0.05$ versus control.

exposed to the hypoxic conditions. This effect was possibly due to the increased $[Ca^{2+}]_i$ recorded in the reoxygenation phase in the presence of BED in comparison to the reoxygenation phase alone, thus reinforcing the importance of NCX3 in buffering $[Ca^{2+}]_i$ under hypoxic conditions. Accordingly, the damage of CA3 area in organotypic cultures was particularly exacerbated during OGD in the presence of BED. However, no significant effect of the drug was observed in CA1 and DG hippocampal sub regions exposed to OGD. This different vulnerability of CA3 region to NCX3 inhibition exerted by BED might be ascribed to the greater expression of this isoform in CA3 compared with CA1 and DG sub regions.[3,16] Furthermore, BED, icv administered, dramatically increased the extent of the ischemic lesion in rats after MCAO followed by reperfusion, thus producing the impairment of several functions. Accordingly, mice lacking ncx3 gene exhibit reduced motor activity, weakness of forelimb muscles, and fatigability in comparison with $ncx3^{+/+}$ mice.[22] Furthermore, ncx3−/− mice exhibit hypomyelination that is accompanied by a reduction of spinal cord size[23,24] and displays an impairment in hippocampal long-term potentiation and spatial learning and memory.[25] At the cellular level, NCX3 extrudes Ca^{2+} from mitochondria, thus protecting neurons exposed to hypoxic conditions.[26] Furthermore, in the same experimental conditions, BHK cells singly transfected with NCX3 show a greater resistance to hypoxia plus reoxygenation, maintaining the ability to buffer intracellular Ca^{2+} overload.[14] This property might be correlated with the ability of NCX3 to operate, unlike the other two NCX isoforms expressed in the brain, NCX1 and NCX2, even when ATP levels are reduced.[14] As matter of fact, the three NCX isoforms display a different sensitivity to ATP levels.[27] In particular, during ATP depletion, NCX1 and NCX2 isoform activity is reduced, whereas NCX3 is still operative.[27] In agreement with this specific function proposed for NCX3, our previous experiments in vivo, entailing the induction of permanent middle cerebral artery occlusion in rats, have demonstrated that NCX3 mRNA is upregulated 24 h after the injury in brain regions belonging to the periinfarct area.[28] This NCX3 upregulation, as opposed to NCX2 downregulation, has been interpreted as a compensatory mechanism that counterbalances the reduced activity of NCX2 protein, thus counteracting the dysregulation of $[Ca^{2+}]_i$ homeostasis in the surviving neurons of the penumbra zone.[28] This suggests a crucial role of neuronal NCX3 isoform in modulating $[Ca^{2+}]_i$ homeostasis under hypoxic conditions. Collectively, the results obtained in the present research work indicate that BED is the most potent

DOI: 10.1021/acschemneuro.5b00043
ACS Chem. Neurosci. 2015, 6, 1361−1370

and selective inhibitor of NCX3 so far identified, and suggest that this compound may represent a useful tool to dissect the differential role played by NCX3 isoform in all those diseases that require a tight control of Ca^{2+} homeostasis through NCX3 function.

METHODS

Cell Culture, Cortical Neurons, and Organotypic Hippocampal Slice Cultures. Stably transfected Baby Hamster Kidney (BHK) cells with canine cardiac NCX1, rat brain NCX2, or NCX3 were grown on plastic dishes in a mix of DMEM and Ham's F12 media (1:1) (Invitrogen, MI, Italy) supplemented with 5% fetal bovine serum, 100 U/mL penicillin, and 100 μg/mL streptomycin (Sigma, St. Louis, MO).[14] Cortical neurons were prepared from brains of 16-day-old Wistar rat embryos (Charles River) as previously reported[29,33] and used at 7−10 days in vitro. Cells were cultured in a humidified 5% CO_2 atmosphere, and the culture medium was changed every 2 days. For microfluorimetric and electrophysiological studies, cells were seeded on glass coverslips (Fisher, Springfield, NJ) coated with poly-L-lysine (30 μg/mL) (Sigma, St. Louis, MO) and used at least 12 h after seeding. Organotypic hippocampal slice cultures (OHSCs) were prepared as previously described.[30] Briefly, 400 μm thick coronal brain slices from P5−P7 mouse pups were used. To increase the reproducibility of the data, two consecutive slices from the two hippocampi of the same animal were always dissected at the same level in all the experimental groups. Slices were grown on semi permeable filter inserts (Millipore, GIBCO, Italy) in six-well plates containing culture medium (50% minimum essential medium, 25% Hank's balanced salt solution, 25% heat inactivated horse serum, 5 mg/mL glucose, 1 mM glutamine, 1% Fungizone). The culture period was 14 days in vitro.

Generation and Stable Expression of Wild-Type and Mutant Exchangers. BHK cell lines, expressing dog heart NCX1.1, rat brain NCX2.1 and NCX3.3 were generous gift from Dr. Kenneth Philipson (UCLA, Los Angeles, CA). Deletion mutant NCX3, NCX3Δf, was obtained deleting amino acidic region 292−708 of rat brain NCX3 cDNA by means of quikchange site-directed mutagenesis kit (Stratagene, Italy). cDNA of NCX1/NCX3 chimeras were obtained from Dr. Takahiro Iwamoto (Fukuoka University, Japan). To stably express chimeric and mutant exchangers, pKCRH or pCEFL plasmids carrying exchanger cDNAs were transfected in the presence of Lipofectamine 2000 (Invitrogen, Italy) into wild-type BHK cell line. Cell clones highly expressing Na^+/Ca^{2+} exchange activity were selected by a Ca^{2+}-killing procedure with the Ca^{2+} ionophore Ionomycin. In the presence of this ionophore, cells not expressing the exchanger died for Ca^{2+} overload.[31]

$[Ca^{2+}]_i$ Measurement. $[Ca^{2+}]_i$ was measured by single cell computer-assisted video imaging as previously shown.[14] Briefly, BHK cells, grown on glass coverslips, were loaded with 6 μM Fura-2 acetoxymethyl ester (Fura-2AM) for 30 min at 37 °C in normal Krebs solution containing the following (in mM): 5.5 KCl, 160 NaCl, 1.2 $MgCl_2$, 1.5 $CaCl_2$, 10 glucose, and 10 Hepes-NaOH, pH 7.4. At the end of the Fura-2AM loading period, the coverslips were placed into a perfusion chamber (Medical System, Co. Greenvale, NY) mounted onto the stage of an inverted Zeiss Axiovert 200 microscope (Carl Zeiss, Germany) equipped with a FLUAR 40× oil objective lens. The experiments were carried out with a digital imaging system composed of a MicroMax 512BFT cooled CCD camera (Princeton Instruments, Trenton, NJ, USA), LAMBDA 10-2 filter wheeler (Sutter Instruments, Novato, CA), and Meta-Morph/MetaFluor Imaging System software (Universal Imaging, West Chester, PA). After loading, cells were alternatively illuminated at wavelengths of 340 and 380 nm by a xenon lamp. The emitted light was passed through a 512 nm barrier filter. Fura-2 fluorescence intensity was measured every 3 s. Forty to sixty-five individual cells were selected and monitored simultaneously from each coverslip. All the results are presented as cytosolic Ca^{2+} concentration. Assuming that the KD for FURA-2 was 224 nM, the equation of Grynkiewicz[32] was used for calibration. NCX activity, shown NCX reverse mode was determined by switching the normal Krebs medium to Na^+-deficient $NMDG^+$ medium (Na^+-free) (in mM): 5.5 KCl, 147 *N*-methyl glucamine, 1.2 $MgCl_2$, 1.5 $CaCl_2$, 10 glucose, and 10 Hepes-NaOH (pH 7.4).[14,33]

Measurement of Na^+-Dependent $^{45}Ca^{2+}$ Uptake and $^{45}Ca^{2+}$ Efflux. $^{45}Ca^{2+}$ influx into the cells was measured by the method previously described.[14] After treatments, cells cultured in 24-well dishes were incubated in normal Krebs (in mM): 5.5 KCl, 145 NaCl, 1.2 $MgCl_2$, 1.5 $CaCl_2$, 10 glucose, and 10 Hepes-NaOH, pH 7.4 containing 1 mM ouabain and 10 μM monensin at 37 °C for 10 min. Then, $^{45}Ca^{2+}$ uptake was initiated by switching the normal Krebs medium to Na^+-free NMDG (in mM): 5.5 KCl, 147 *N*-methyl D-glucamine (NMDG), 1.2 $MgCl_2$, 1.5 $CaCl_2$, 10 glucose, and 10 Hepes-NaOH (pH 7.4) containing 10 μM $^{45}Ca^{2+}$ (74 KBq/mL) and 1 mM ouabain. After 30 s incubation, cells were washed with an ice-cold solution containing 2 mM La^{3+} to stop $^{45}Ca^{2+}$ uptake. Cells were subsequently solubilized with 0.1 N NaOH and aliquots were taken to determine radioactivity and protein content.[34] To measure $^{45}Ca^{2+}$ efflux, cells were loaded with 1 μM $^{45}Ca^{2+}$ (74 KBq/mL) together with 1 μM ionomycin for 60 s in normal Krebs. Next, cells were exposed either to a Ca^{2+}- and Na^+-free solution (a condition that blocks both intracellular $^{45}Ca^{2+}$ efflux and extracellular Ca^{2+} influx) or to a Ca^{2+}-free plus 2 mM EGTA containing 145 mM Na^+ (a condition that promotes $^{45}Ca^{2+}$ efflux). Thapsigargin at 1 μM was present in both solutions. $^{45}Ca^{2+}$ efflux was started by using Ca^{2+}-free-Na^+ containing solution plus 2 mM EGTA. Cells were exposed to this solution, which promotes $^{45}Ca^{2+}$ efflux, for 10 s. At the time chosen (10 s), no efflux was detected in BHK-Wilde cells. Na_0^+-dependent $^{45}Ca^{2+}$ efflux was estimated by subtracting $^{45}Ca^{2+}$ efflux in Ca^{2+}- and Na^+-free from that in Ca^{2+}-free solution. Cells were subsequently solubilized with 0.1 N NaOH, and aliquots were taken to determine radioactivity and protein content by Bradford method.[34]

Electrophysiology. All currents were recorded by patch-clamp technique in whole-cell configuration using a Digidata 1322A interface (Molecular Devices). Data were acquired and analyzed using the pClamp software (version 9.0, Molecular Devices). The currents were recorded by fire-polished borosilicate electrodes with a final resistance of 2.5−4 MΩ filled with a specific internal solution. I_{NCX} filtered at 5 kHz was recorded from BHK wild type (Wt) and BHK-NCX1, -NCX2, and -NCX3 stably transfected cells.[10,15] Briefly, I_{NCX} was recorded starting from a holding potential of −60 mV up to a short-step depolarization at +60 mV (60 ms).[35] Then, a descending voltage ramp from +60 to −120 mV was applied. The current recorded in the descending portion of the ramp (from +60 to −120 mV) was used to plot the current−voltage (*I*−*V*) relation curve. The magnitudes of I_{NCX} were measured at the end of +60 mV (reverse mode) and at the end of −120 mV (forward mode), respectively. The Ni^{2+}-insensitive components were subtracted from total currents to isolate I_{NCX}. External Ringer solution contained (in mM): 126 NaCl, 1.2 $NaHPO_4$, 2.4 KCl, 2.4 $CaCl_2$, 1.2 $MgCl_2$, 10 glucose and 18 $NaHCO_3$, 20 TEA, 10 nM TTX, and 10 μM nimodipine (pH 7.4). The dialysing pipet solution contained (mM): 100 K-gluconate, 10 tetraethylammonium (TEA), 20 NaCl, 1 Mg-ATP, and 0.1 $CaCl_2$, 2 $MgCl_2$, 0.75 EGTA, Hepes 10, adjusted to pH 7.2 with CsOH. TEA (20 mM) and Cs were included to block delayed outward rectifier K^+ components, nimodipine (10 μM) and TTX (50 nM) were added to external solution to block L-type Ca-channels and TTX-sensitive Na^+-channels, respectively. I_{NCX} values were normalized for membrane capacitance. TTX-sensitive Na^+ currents were recorded in pituitary GH_3 cells as previously shown.[15] For TTX-sensitive Na^+ channel recordings, pituitary GH_3 cells were perfused with an extracellular Ringer solution containing 20 mM TEA and 5 μM nimodipine. The pipettes were filled with (in mM): 110 CsCl, 10 TEA, 2 $MgCl_2$, 10 EGTA, 8 glucose, 2 Mg-ATP, 0.25 cAMP, and 10 HEPES, pH 7.3. TTX-sensitive Na^+-currents were recorded by applying, from an holding potential of −70 mV, depolarizing voltage steps of 50 ms duration in 10 mV from −100 to +50 mV elicited at 0.066 Hz frequency (1 pulse every 15 s). The current−voltage relationship of Na^+ currents were obtained normalizing the peak value for the membrane voltage imposed during the step.

DOI: 10.1021/acschemneuro.5b00043
ACS Chem. Neurosci. 2015, 6, 1361−1370

Oxygen and Glucose Deprivation. Hypoxic conditions were induced by exposing hippocampal cultures to oxygen- and glucose-free medium in a humidified atmosphere containing 95% nitrogen and 5% CO_2.[36] After 25 min of OGD followed by 24 h of reoxygenation, cell injury was assessed using the fluorescent dye propidium iodide (PI) (Invitrogen). Its uptake was recorded with a digital camera (Media Cybernetics, Silver Springs, MD) mounted on a Nikon Eclipse 400 fluorescence microscope (Nikon Instruments, Florence, Italy). For densitometric measurements, the digital photos were analyzed with the Image Pro-Plus software (Media Cybernetics), after freehand outlining of the CA1, CA3, and dentate gyrus (DG) neuronal layers was performed as previously described.[37] Densitometric data were obtained by an integrated algorithm that considers the mean of optical density.[30] In primary cortical neurons, cell injury was assessed after 3 h of OGD followed by 21 h of reoxygenation. PI (7 μM) and fluorescein diacetate (FDA; 36 μM) positive cells were counted in three representative high-power fields of independent cultures, and cell death was determined by the ratio of the number of PI-positive cells/PI FDA positive cells.

Experimental Groups for in Vivo Studies. C57/BL6 mice (Charles River, Italy) aged between 6 and 8 weeks and weighing 27−30 g were housed under diurnal lighting conditions. Experiments were performed according to the international guidelines for animal research and approved by the Animal Care Committee of "Federico II", University of Naples, Italy.

Transient Middle-Cerebral Artery Occlusion Model (tMCAo). Mice were subjected to tMCAo as previously described.[38] A 5-0 nylon filament was inserted through the external carotid artery stump and advanced into the left internal carotid artery until it blocked the origin of the middle cerebral artery (MCA). After 60 min MCA occlusion, the filament was withdrawn to restore blood flow.

Monitoring of Blood Gas Concentration and Cerebral Blood Flow (CBF) with Laser-Doppler Flowmetry. A catheter was inserted into the femoral artery to measure arterial blood gases before and after ischemia (Rapid lab 860; Chiron Diagnostic). CBF was monitored in the cerebral cortex ipsilateral to the occluded MCA with a laser-Doppler flowmeter (Periflux system, 5000). Once a stable CBF signal was obtained, the MCA was occluded. CBF monitoring was continued up to 30 min after the end of the surgical procedure, when the occurred reperfusion was verified.

Evaluation of the Ischemic Volume. Mice were sacrificed 24 h after ischemia. Ischemic volume was evaluated by 2,3,5-triphenyl tetrazolium chloride (TTC) staining.[39] The infarct area was calculated with image analysis software (Image-Pro Plus).[3] The total infarct volume was expressed as percentage of the volume of the hemisphere ipsilateral to the lesion.[3] Ischemic volumes were evaluated in a blind manner.

Drugs, Statistical Analysis, and Determination of IC_{50}'s. BED was solubilized in dimethyl sulfoxide at concentrations of 1 mM, and stock solutions were kept at −20 °C. Appropriate drug dilutions were prepared daily. Statistical analysis was performed with 2-way ANOVA, followed by Newman-Keuel's test. Statistical significance was accepted at the 95% confidence level ($p < 0.05$). Values are expressed as means ± SEM. To obtain IC_{50}'s of BED, all data were fitted to the following binding isotherm: $y = \max/(1 1X/IC_{50})n$, where X is the drug concentration and n is the Hill coefficient.

AUTHOR INFORMATION

Corresponding Author

*Telephone: +39-81-7463318. Fax: +39-81-7463323. E-mail: lannunzi@unina.it.

Author Contributions

‖A. Secondo and G. Pignataro contributed equally to this work. A. Secondo, G. Pignataro, V. Santagada, G. Caliendo, G. Di Renzo, and L. Annunziato participated in research design. A. Secondo, P. Ambrosino, A. Pannaccione, P. Molinaro, M. Cantile, F. Boscia, A. Esposito, O. Cuomo, M. J. Sisalli, A. Scorziello, N. Guida, S. Anzillotti, B. Severino, and F. Fiorino conducted experiments. G. Pignataro, A. Secondo, P. Ambrosino, A. Pannaccione, and F. Boscia performed data analysis. A. Secondo, G. Pignataro, G. Di Renzo, and L. Annunziato wrote or contributed to the writing of the manuscript.

Funding

This work was supported by PON03PE_00146_1 by MIUR, Progetto Giovani Ricercatori GR-2010-2318138 from Ministero della Salute to A. Secondo, FISM 2012/R/1 to F. Boscia, and Futuro in Ricerca MIUR (RBFR13M6FN) to P. Molinaro.

Notes

The authors declare no competing financial interest.

ACKNOWLEDGMENTS

We thank Dr. Paola Merolla for editorial revision.

REFERENCES

(1) Philipson, K. D., and Nicoll, D. A. (2000) Sodium-calcium exchange: A molecular perspective. *Annu. Rev. Physiol. 62*, 111−133.

(2) Annunziato, L., Pignataro, G., and Di Renzo, G. F. (2004) Pharmacology of brain Na^+-Ca^{2+} exchanger: from molecular biology to therapeutic perspectives. *Pharmacol. Rev. 56*, 633−654.

(3) Pignataro, G., Gala, R., Cuomo, O., Tortiglione, A., Giaccio, L., Castaldo, P., Sirabella, R., Matrone, C., Canitano, A., Amoroso, S., Di Renzo, G., and Annunziato, L. (2004) Two sodium/calcium exchanger gene products, NCX1 and NCX3, play a major role in the development of permanent focal cerebral ischemia. *Stroke 35*, 2566−2570.

(4) Molinaro, P., Cuomo, O., Pignataro, G., Boscia, F., Sirabella, R., Pannaccione, A., Secondo, A., Scorziello, A., Adornetto, A., Gala, R., Viggiano, D., Sokolow, S., Herchuelz, A., Schurmans, S., Di Renzo, G., and Annunziato, L. (2008) Targeted disruption of Na^+-Ca^{2+} exchanger 3 (NCX3) gene leads to a worsening of ischemic brain damage. *J. Neurosci. 28*, 1179−1184.

(5) Ren, X., and Philipson, K. D. (2013) The topology of the cardiac Na^+/Ca^{2+} exchanger, NCX1. *J. Mol. Cell. Cardiol. 57*, 68−71.

(6) Nicoll, D. A., Longoni, S., and Philipson, K. D. (1990) Molecular cloning and functional expression of the cardiac sarcolemmal Na^+-Ca^{2+} exchanger. *Science 250*, 562−5.

(7) Li, Z., Matsuoka, S., Hryshko, L. V., Nicoll, D. A., Bersohn, M. M., Burke, E. P., Lifton, R. P., and Philipson, K. D. (1994) Cloning of the NCX2 isoform of the plasma membrane Na^+-Ca^{2+} exchanger. *J. Biol. Chem. 269*, 17434−17439.

(8) Nicoll, D. A., Quednau, B. D., Qui, Z., Xia, Y. R., Lusis, A. J., and Philipson, K. D. (1996) Cloning of a third mammalian Na^+/Ca^{2+} exchanger, NCX3. *J. Biol. Chem. 271*, 24914−24921.

(9) Nicoll, D. A., Ottolia, M., Lu, L., Lu, Y., and Philipson, K. D. (1999) A new topological model of the cardiac sarcolemmal Na^+/Ca^{2+} exchanger. *J. Biol. Chem. 274*, 910−917.

(10) Secondo, A., Molinaro, P., Pannaccione, A., Esposito, A., Cantile, M., Lippiello, P., Sirabella, R., Iwamoto, T., Di Renzo, G., and Annunziato, L. (2011) Nitric oxide stimulates NCX1 and NCX2 but inhibits NCX3 isoform by three distinct molecular determinants. *Mol. Pharmacol. 79*, 558−568.

(11) Sharikabad, M. N., Cragoe, E. J., and Brors, O. (1997) Inhibition by 5-*N*-(4-chlorobenzyl)-2′,4′-dimethylbenzamil of Na^+-Ca^{2+} exchange and L-type Ca^{2+} channels in isolated cardiomyocytes. *Pharmacol. Toxicol. 80*, 57−61.

(12) Kaczorowski, G. J., Slaughter, R. S., King, V. F., and Garcia, M. L. (1989) Inhibitors of sodium-calcium exchange: Identification and development of probes of transport activity. *Biochim. Biophys. Acta 988*, 287−302.

(13) Fiorino, F., Eiden, M., Giese, A., Severino, B., Esposito, A., Groschup, M. H., Perissutti, E., Magli, E., Incisivo, G. M., Ciano, A., Frecentese, F., Kretzschmar, H. A., Wagner, J., Santagada, V., and Caliendo, G. (2012) Synthesis of benzamide derivatives and their evaluation as antiprion agents. *Bioorg. Med. Chem. 20*, 5001−5011.

DOI: 10.1021/acschemneuro.5b00043
ACS Chem. Neurosci. 2015, 6, 1361−1370

(14) Secondo, A., Staiano, R. I., Scorziello, A., Sirabella, R., Boscia, F., Adornetto, A., Valsecchi, V., Molinaro, P., Canzoniero, L. M., Di Renzo, G., and Annunziato, L. (2007) BHK cells transfected with NCX3 are more resistant to hypoxia followed by reoxygenation than those transfected with NCX1 and NCX2: Possible relationship with mitochondrial membrane potential. *Cell Calcium 42*, 521−535.
(15) Secondo, A., Pannaccione, A., Molinaro, P., Ambrosino, P., Lippiello, P., Esposito, A., Cantile, M., Khatri, P. R., Melisi, D., Di Renzo, G., and Annunziato, L. (2009) Molecular pharmacology of the amiloride analog 3-amino-6-chloro-5-[(4-chloro-benzyl)amino]-*n*-[[(2,4-dimethylbenzyl)-amino]iminomethyl]-pyrazinecarboxamide (CB-DMB) as a pan inhibitor of the Na^+-Ca^{2+} exchanger isoforms NCX1, NCX2, and NCX3 in stably transfected cells. *J. Pharmacol. Exp. Ther. 331*, 212−21.
(16) Papa, M., Canitano, A., Boscia, F., Castaldo, P., Sellitti, S., Porzig, H., Taglialatela, M., and Annunziato, L. (2003) Differential expression of the Na^+-Ca^{2+} exchanger transcripts and proteins in rat brain regions. *J. Comp. Neurol. 461*, 31−48.
(17) Matsuda, T., Arakawa, N., Takuma, K., Kishida, Y., Kawasaki, Y., Sakaue, M., Takahashi, K., Takahashi, T., Suzuki, T., Ota, T., Hamano-Takahashi, A., Onishi, M., Tanaka, Y., Kameo, K., and Baba, A. (2001) SEA0400, a novel and selective inhibitor of the Na^+-Ca^{2+} exchanger, attenuates reperfusion injury in the in vitro and in vivo cerebral ischemic models. *J. Pharmacol. Exp. Ther. 298*, 249−256.
(18) Iwamoto, T., and Kita, S. (2006) YM-244769, a novel Na^+-Ca^{2+} exchange inhibitor that preferentially inhibits NCX3, efficiently protects against hypoxia/reoxygenation-induced SH-SY5Y neuronal cell damage. *Mol. Pharmacol. 70*, 2075−2083.
(19) Ryan, C., Shaw, G., and Hardwicke, P. M. (2007) Effect of Ca^{2+} on protein kinase A-mediated phosphorylation of a specific serine residue in an expressed peptide containing the Ca2+-regulatory domain of scallop muscle Na+-Ca2+ exchanger. *Ann. N.Y. Acad. Sci. 1099*, 43−52.
(20) Molinaro, P., Cantile, M., Cuomo, O., Secondo, A., Pannaccione, A., Ambrosino, P., Pignataro, G., Fiorino, F., Severino, B., Gatta, E., Sisalli, M. J., Milanese, M., Scorziello, A., Bonanno, G., Robello, M., Santagada, V., Caliendo, G., Di Renzo, G., and Annunziato, L. (2013) Neurounina-1, a novel compound that increases Na+-Ca2+ exchanger activity, effectively protects against stroke damage. *Mol. Pharmacol. 83*, 142−156.
(21) Iwamoto, T. (2007) Na^+-Ca^{2+} exchange as a drug target−insights from molecular pharmacology and genetic engineering. *Ann. N.Y. Acad. Sci. 1099*, 516−28.
(22) Sokolow, S., Manto, M., Gailly, P., Molgo, J., Vandebrouck, C., Vanderwinden, J. M., Herchuelz, A., and Schurmans, S. (2004) Impaired neuromuscular transmission and skeletal muscle fiber necrosis in mice lacking Na/Ca exchanger 3. *J. Clin. Invest. 113*, 265−273.
(23) Boscia, F., D'Avanzo, C., Pannaccione, A., Secondo, A., Casamassa, A., Formisano, L., Guida, N., Sokolow, S., Herchuelz, A., and Annunziato, L. (2012) Silencing or knocking out the Na^+-Ca^{2+} exchanger-3 (NCX3) impairs oligodendrocyte differentiation. *Cell Death Differ. 19*, 562−572.
(24) Annunziato, L., Boscia, F., and Pignataro, G. (2013) Ionic transporter activity in astrocytes, microglia, and oligodendrocytes during brain ischemia. *J. Cereb. Blood Flow Metab. 33*, 969−982.
(25) Molinaro, P., Viggiano, D., Nistico, R., Sirabella, R., Secondo, A., Boscia, F., Pannaccione, A., Scorziello, A., Mehdawy, B., Sokolow, S., Herchuelz, A., Di Renzo, G. F., and Annunziato, L. (2012) Na^+-Ca^{2+} exchanger (NCX3) knock-out mice display an impairment in hippocampal long-term potentiation and spatial learning and memory. *J. Neurosci. 31*, 7312−7321.
(26) Scorziello, A., Savoia, C., Sisalli, M. J., Adornetto, A., Secondo, A., Boscia, F., Esposito, A., Polishchuk, E. V., Polishchuk, R. S., Molinaro, P., Carlucci, A., Lignitto, L., Di Renzo, G., Feliciello, A., and Annunziato, L. (2013) NCX3 regulates mitochondrial Ca^{2+} handling through the AKAP121-anchored signaling complex and prevents hypoxia-induced neuronal death. *J. Cell Sci. 126*, 5566−5577.
(27) Linck, B., Qiu, Z., He, Z., Tong, Q., Hilgemann, D. W., and Philipson, K. D. (1998) Functional comparison of the three isoforms of the Na^+-Ca^{2+} exchanger (NCX1, NCX2, NCX3). *Am. J. Physiol. 274*, C415−C423.
(28) Boscia, F., Gala, R., Pignataro, G., de Bartolomeis, A., Cicale, M., Ambesi-Impiombato, A., Di Renzo, G., and Annunziato, L. (2006) Permanent focal brain ischemia induces isoform-dependent changes in the pattern of Na^+-Ca^{2+} exchanger gene expression in the ischemic core, periinfarct area, and intact brain regions. *J. Cereb. Blood Flow Metab. 26*, 502−517.
(29) Scorziello, A., Pellegrini, C., Forte, L., Tortiglione, A., Gioielli, A., Iossa, S., Amoroso, S., Tufano, R., Di Renzo, G., and Annunziato, L. (2001) Differential vulnerability of cortical and cerebellar neurons in primary culture to oxygen glucose deprivation followed by reoxygenation. *J. Neurosci. Res. 63*, 20−26.
(30) Boscia, F., Annunziato, L., and Taglialatela, M. (2006) Retigabine and flupirtine exert neuroprotective actions in organotypic hippocampal cultures. *Neuropharmacology 51*, 283−294.
(31) Iwamoto, T., Wakabayashi, S., Imagawa, T., and Shigekawa, M. (1998) Na^+-Ca^{2+} exchanger overexpression impairs calcium signaling in fibroblasts: inhibition of the $[Ca^{2+}]$ increase at the cell periphery and retardation of cell adhesion. *Eur. J. Cell. Biol. 76*, 228−236.
(32) Grynkiewicz, G., Poenie, M., and Tsien, R. Y. (1985) A new generation of Ca^{2+} indicators with greatly improved fluorescence properties. *J. Biol. Chem. 260*, 3440−3450.
(33) Sirabella, R., Secondo, A., Pannaccione, A., Scorziello, A., Valsecchi, V., Adornetto, A., Bilo, L., Di Renzo, G., and Annunziato, L. (2009) Anoxia-induced NF-kappaB-dependent upregulation of NCX1 contributes to Ca^{2+} refilling into endoplasmic reticulum in cortical neurons. *Stroke 40*, 922−929.
(34) Bradford, M. M. (1976) A rapid and sensitive method for the quantitation of microgram quantities of protein utilizing the principle of protein-dye binding. *Anal. Biochem. 72*, 248−254.
(35) He, L. P., Cleemann, L., Soldatov, N. M., and Morad, M. (2003) Molecular determinants of cAMP-mediated regulation of the Na^+-Ca^{2+} exchanger expressed in human cell lines. *J. Physiol. 548*, 677−689.
(36) Scorziello, A., Santillo, M., Adornetto, A., Dell'aversano, C., Sirabella, R., Damiano, S., Canzoniero, L. M., Renzo, G. F., and Annunziato, L. (2007) NO-induced neuroprotection in ischemic preconditioning stimulates mitochondrial Mn-SOD activity and expression via Ras/ERK1/2 pathway. *J. Neurochem. 103*, 1472−1480.
(37) Boscia, F., Ferraguti, F., Moroni, F., Annunziato, L., and Pellegrini-Giampietro, D. E. (2008) mGlu1alpha receptors are co-expressed with CB1 receptors in a subset of interneurons in the CA1 region of organotypic hippocampal slice cultures and adult rat brain. *Neuropharmacology 55*, 428−439.
(38) Longa, E. Z., Weinstein, P. R., Carlson, S., and Cummins, R. (1989) Reversible middle cerebral artery occlusion without craniectomy in rats. *Stroke 20*, 84−91.
(39) Bederson, J. B., Pitts, L. H., Germano, S. M., Nishimura, M. C., Davis, R. L., and Bartkowski, H. M. (1986) Evaluation of 2,3,5-triphenyltetrazolium chloride as a stain for detection and quantification of experimental cerebral infarction in rats. *Stroke 17*, 1304−1308.

DOI: 10.1021/acschemneuro.5b00043
ACS Chem. Neurosci. 2015, 6, 1361−1370